Letter

Remote activation of a nanopore for high performance genetic detection using a pH taxis-mimicking mechanism

Yong Wang, Kai Tian, Xiao Du, Ruicheng Shi, and Li-Qun Gu

Anal. Chem., **Just Accepted Manuscript** • DOI: 10.1021/acs.analchem.7b03979 • Publication Date (Web): 28 Nov 2017

Remote activation of a nanopore for high performance genetic detection using a pH taxis-mimicking mechanism

Yong Wang[1]*, Kai Tian[2], Xiao Du[2], Rui-Cheng Shi[2] and Li-Qun Gu[2]*

[1]Virginia G. Piper Biodesign Center for Personalized Diagnostics, The Biodesign Institute, Arizona State University, Tempe, AZ 85287. [2]Department of Bioengineering and Dalton Cardiovascular Research Center, University of Missouri, Columbia, MO 65211.

ABSTRACT: Aerolysin protein pore has been widely used for sensing peptides and proteins. But only a few groups explored this nanopore for nucleic acids detection. The challenge is the extremely low capture efficiency for nucleic acids (>10 bases), which severely lowers the sensitivity of an aerolysin-based genetic biosensor. Here we reported a simple and easy-to-operate approach to non-covalently transform aerolysin into a highly nucleic acids-sensitive nanopore. Through a remote pH-modulation mechanism, we simply lower the pH on one side of the pore, then aerolysin is immediately "activated" and enabled to capture target DNA/RNA efficiently from the opposite side of the pore. This mechanism also decelerates DNA translocation, a desired property for sequencing and gene detection, allowing temporal separation of DNAs in different lengths. This method provides insight into the nanopore engineering for biosensing, making aerolysin applicable in genetic and epigenetic detections of long nucleic acids.

Nanopore is a new-generation biosensing technology. Its single-molecule sensitivity enables a variety of biomedical applications[1-2], from gene sequencing[3-4] to genetic, epigenetic[5-10] and proteomic detections[11-20]. Recently, aerolysin has been emerged as a new nanopore system for sensing peptides[21-22], proteins[23-27], polysaccharides[28], and biological relevant polymers[29]. However, in contrast to most protein pores (e.g. Phi29[16], MspA[4], α-hemolysin[30] and SP1[31]), there are much fewer studies on applying aerolysin in nucleic acid detections. These studies include, Pastoriza-Gallego et al (2014)[32] and Payet et al (2015)[33] studied the translocation of DNA through the aerolysin pore; and the Long's group (2016)[34] discovered that aerolysin's conductance variation can discriminate the length of short oligonucleotides (<10 nts) at the single nucleotide resolution. By now a main challenge confronted by aerolysin for genetic detection is the extremely low capture efficiency for target nucleic acids (>10 nts). For example, previous studies[32-33] show that, DNA cannot be captured by aerolysin at voltage <100 mV, and DNA translocation rate at voltage >100 mV is tens of folds lower compared with the widely applied α-hemolysin pore. Such low capture efficiency is impractical for nucleic acids detection, and lowers the enthusiasm for developing aerolysin-based genetic biosensor. In this letter, we presented an interesting non-covalent approach to transforming aerolysin into a highly nucleic acids-sensitive nanopore through a remote pH modulation mechanism. The "activated" aerolysin can not only efficiently capture gene fragments, but also decelerate nucleic acids translocation through the nanopore. Both properties are required for sequencing and precise genetic detection.

As shown in Fig. 1a, we formed single aerolysin pores from the *cis* side of the lipid bilayer, and presented target DNA D16 (16-nt, Table S1) in the *cis* solution. A positive voltage (+40 mV and +80 mV) was applied from the *trans* compartment, with *cis* grounded, to drive *cis* DNA toward the pore. The current trace in Fig. 1a shows that when both *cis* and *trans* solutions were neutral, the nanopore conductance was not affected by D16, indicating that *cis* DNA cannot access the aerolysin pore. Strikingly, when lowering pH of the *trans* solution to 3.4 while keeping the *cis* solution (where DNA was presented) neutral, we immediately observed a large number of current blockades that reduced the current from I_0 of the empty pore to I with I/I_0=4.3% (Fig. S1). The block frequency increased in proportion to the *cis* DNA concentration (Fig. S2). Without DNA, aerolysin alone in this pH gradient did not generate blocks (Fig. S3). These findings together suggest that the blockades appeared at low *trans* pH are produced by capturing DNA from the *cis* entrance.

This pH effect on DNA capture also applied to DNA in the *trans* solution (Fig. S4). *Trans* D16 did not affect the pore

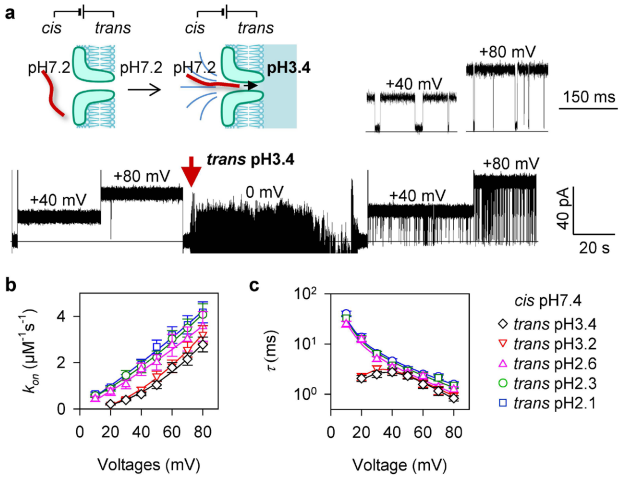

Figure 1 Activation of aerolysin by acidic solution on one side to capture DNA from the other side capture and translocation. **a.** Model (up) and current trace (bottom) showing that DNA D16 (1 μM) on *cis* side cannot be captured by aerolysin when both *cis* and *trans* solutions were at pH7.4 (left), and can immediately produce a large number of current blocks when *trans* solution was changed to pH3.4 while *cis* solution remained pH7.4 (right); **b** and **c.** Voltage-dependence of DNA capture rate (k_{on}, b) and block duration (τ, c) at various acidic *trans* pH (Fig. S10a-e for histograms.

conductance in neutral solutions on both sides, but produced many blockades as the *cis* pH was lowered to 2.6 while the *trans* pH (where DNA was presented) remained neutral, suggesting that low *cis* pH enables DNA capture from the *trans* entrance. We also found that a RNA fragment can also be captured from one side (*cis*) by lowing pH of the opposite side (*trans*) (Fig. S5). Overall, we conclude that, by increasing the acidity on one side, aerolysin can be remotely "activated" and enabled to capture nucleic acids from the opposite side.

Fig. 1b shows that, for all *trans* pH tested, the *cis* DNA capture rate (k_{on}) can be enhanced by the voltage. For example, k_{on} for *trans* pH3.4 was increased by over 10 folds from 0.21±0.03 $\mu M^{-1}s^{-1}$ to 2.8±0.4 $\mu M^{-1}s^{-1}$ as voltage increased from +20 mV to +80 mV. This capture efficiency is superior to that of the α-hemolysin pore, which is at the 1 $\mu M^{-1}s^{-1}$ level at +100 mV[35] and close to zero at +80 mV. Studying the voltage-dependence of the capture rate can help to understand the nature of the capture procedure. In a capture event, a DNA molecule first migrates from the bulk solution to the pore opening. This is a diffusive step biased by an electric field outside the pore entrance[36-38]. It is characterized by a linear k_{on}–V relation[9, 36-37]. Next, the DNA is threaded into the pore for translocation, a step that needs to overcome an energy barrier due to the nanopore confinement of DNA end and/or DNA–pore interactions[9, 36-37]. This barrier-limited capture allows k_{on} to be exponentially changed with the voltage (k_{on}~exp(V))[9, 36-37]. The DNA capture by aerolysin can be considered as both voltage-biased diffusion-limited and barrier-limited procedures, but diffusion plays a more dominative role as *trans* pH decreases, due to better linear fitting of the k_{on}–V curves as *trans* pH decreases (Supplementary S1). This implies that lowering *trans* pH can decrease the barrier for capturing DNA from the *cis* entrance.

Decelerated translocation of nucleic acids through the nanopore is a desirable property for sequencing and high performance genetic detection[39]. This can be achieved by lowering the driving voltage. However, low voltage heavily reduces DNA capture efficiency. Here we found that "activated" aerolysin can prominently decelerate DNA translocation while maintaining high capture efficiency at low voltage (Fig. 1a up-right traces and Fig. 1c). The DNA block duration (τ) varied from 0.83 ms to 40 ms at voltage between +10 ~ +80 mV and *trans* pH3.4 ~ 2.1. This time scale is longer than that for DNA translocation in α-hemolysin (~100 μs) by two or three orders of magnitude. For *trans* pH3.4, we observed a hill-shaped τ–V curve, which suggests that DNA translocates through the pore above the peak voltage (+30 ~ +40 mV), but returns to the *cis* solution at smaller voltages[40]. For *trans* pH2.6 and 2.1, we identified a monotonic τ–V relation, which indicates DNA translocation at all voltages. The *cis*-to-*trans* translocation of DNA was verified by PCR amplification of translocated DNA in the *trans* solution (Fig. S6). At the same voltage, τ was consistently prolonged with lowering *trans* pH. For example, at +80 mV, τ was extended from 0.83±0.1 ms to 1.6±0.2 ms as *trans* pH was lowered from 3.4 to 2.1. The pH effect on τ suggests that, in addition to voltage, other factors may contribute to translocation deceleration[41]. One of factors could be DNA protonation, which occurs on the N3 group of adenine (pKa=3.5) and cytosine (pKa=4.2) (Table S2). The resulting reduction of the negative charge on DNA (Supplementary S2) may assist to slow down translocation.

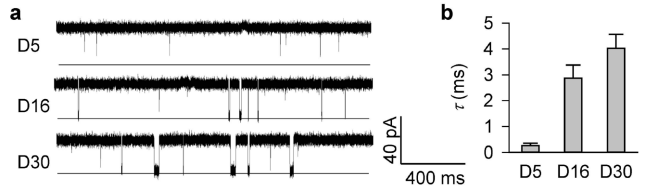

Figure 2 Discriminating DNA of different lengths from their block durations. **a.** Current traces showing DNA blocks in the presence of 1 μM DNAs D5 (5 nts), D16 (16 nts) and D30 (30 nts) (Table S1 for sequences) in the *cis* solution with *cis* pH7.4 vs. *trans* pH3.4, recorded under +40 mV; **b.** Duration of blocks by the three different length DNAs. Histograms for τ are shown in Fig. S11.

Deceleration of DNA translocation allows studying how the DNA translocation time is correlated to the DNA length. The Long's group has found that 2-, 3-, 4-, 5- and 10-base short oligonucleotides can be discriminated in the aerolysin pore based on their characteristic blocking levels[34], but characterization of longer oligonucleotide translocation remains limited in the neutral environment. We detected the translocation time of targets D5, D16, and D30, which contain 5, 16, and 30 nucleotides respectively (Table S1), at *cis* pH7.4 vs *trans* pH3.4, and monitored at +40 mV (Fig. 2). The current traces for the three DNAs show that longer DNA corresponded to longer block duration (Fig. 2a). τ was extended from 0.26±0.09 ms for D5, to 2.9±0.5 ms for D16, and 4.1±0.5 ms for D30 (Fig. 2b), suggesting that longer DNA spends longer time to pass through the pore. The translocation speeds for D5, D16 and D30 were about 19, 5.5, and 7.5 bases per ms. They are in the same scale, but not equal, suggesting that not only the oligonucleotide sequence but also other factors such as the nucleic acids-pore interactions may be involved in the complex translocation procedure. This result indicates the potential for gene fragment length discrimination, which is a long-term interest in our follow-up study.

To understand the remote pH-modulation mechanism, we kept *cis* pH at 7.4 and observed the continuous increase of *cis* DNA capture rate (+40 mV) by lowering *trans* pH from 7.4 to 2.1. As shown in Fig. 3a and b, the DNA capture rate increased in three phases: Initially, k_{on} remained zero from *trans* pH7.4 to 5.0, and modestly increased up to *trans* pH3.7; next, k_{on} sharply climbed up by tens of folds within a narrow pH range from 3.7 to 2.6; finally, k_{on} approximated to saturation as *trans* pH was continuously lowered. The sharp increase of capture rate corresponds to a 1.5 kcal·mol^{-1} activation energy drop from *trans* pH4 to pH2.6 ($RT\cdot\ln(k_{on\text{-}pH2.6}/k_{on\text{-}pH4})$. The k_{on}–*trans* pH correlation can be described using

$$k_{on} = k_{on\_S}/(1 + 10^{trans\ \mathrm{pH}-\mathrm{pH}_{50}}) \qquad (1)$$

where k_{on_S} is the saturate capture rate, and pH_{50} is the *trans* pH at which k_{on} is increased to 50% of k_{on_S}. The fitting gave pH_{50}=3.2. This *trans* pH–dependent capture rate is consistent with the pH-dependent protonation probability, which is governed by the Henderson–Hasselbalch equation,

$$P_{RH} = 1/(1 + 10^{\mathrm{pH}-\mathrm{pKa}}) \qquad (2)$$

where P_{RH} (between 0~1) is the probability of a residue (R) in the protonated state (RH^+), and pKa is the pH value at which

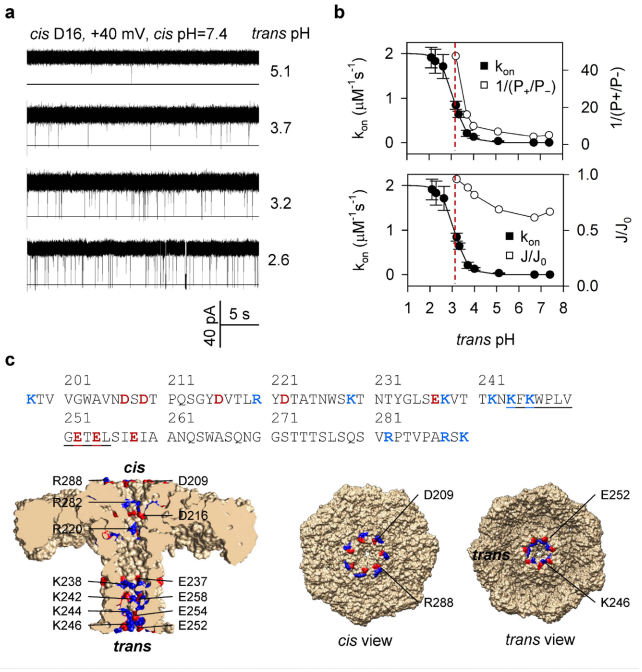

Figure 3 *Trans* pH-dependent capture of *cis* DNA by the aerolysin pore and mechanistic study. **a.** Current traces showing the consistent increase of block frequency for the *cis* DNA D16 (1 μM) as the *trans* pH was lowered from 7.4 to 2.6 (*cis* pH remained 7.4); **b.** D16 capture rate (k_{on}) as the function of the *trans* pH. The k_{on}–*trans* pH curve was fitted using Equation 1. (Top) The *trans* pH-dependent K^+/Cl^- permeability ratio P_+/P_- was shown with the k_{on}–*trans* pH curve (see Fig. S7 for P_+/P_- measurement). (Bottom) *trans* pH-dependent relative net anion flow J/J_0 and the k_{on}–*trans* pH curve. $J=J_-−J_+$ is the net anion flow and J_0 is the maximal anion flow in which the current is completely carried by anions ($J_0=J_-+J_+$). As $P_+/P_-=J_+/J_-$, the permeability ratios were transformed into the relative net ion flow as $J/J_0=(1−P_+/P_-)/(1+P_+/P_-)$; **c.** Aerolysin structure, including cross-section (left), top view (*cis*), bottom view (*trans*), showing charge distribution at the *cis* and *trans* entrance.

P_{RH}=50%. Comparison of Eq. 1 and Eq. 2 suggests that DNA capturing is enhanced by pH-induced protonation.

To prove the occurrence of protonation, we investigated the ion selectivity of aerolysin, supposing that protonation-induced positive charge on the channel wall can produce a net anion (Cl^-) flow. Indeed, Fig. 3b shows that the ratio of the Cl^- vs K^+ flows through aerolysin dramatically increased from 7 folds (K^+/Cl^- permeability ratio P_+/P_-=0.14) in neutral *trans* solution[42] to 16 folds (P_+/P_-=0.06) at *trans* pH3.7, and 50 folds (P_+/P_-=0.02) at *trans* pH3.2 (Fig. S7 for P_+/P_- measurement). Such great enhancement of the net Cl^- flow should be due to the increase of positive charges in the pore, thus verifying the protonation under the pH gradient. Structurally[43-44], the aerolysin pore offers rich protonatable residues on the channel wall and in particular around both entrances (Fig. 3c), such as E237, E252, E254 and E258 close to the *trans* entrance for protonation at low *trans* pH, and D209 and D216 close to the *cis* entrance for protonation at low *cis* pH. Their protonation would induce a large number of net positive charges contributed by K238, K242, K244 and K246 in the *trans* barrel, and/or R220, R282 and R288 around the *cis* entrance, which work together to produce a large net anion flow.

The observed pH-dependent anion flow allows us to propose that there exists a protonation-induced electroosmostic flow that drives DNA capturing by aerolysin. Previously, we have found that engineered α-hemolysin pore with different charge polarities can modulate the pore's ion selectivity; the resulting net ion flow produced a nano-electroosmotic flow to drive neutral molecules binding with the pore.[45] In the current study, Fig. 3b shows that the enhancement of the net Cl^- flow was synchronized with the increase of DNA capture rate as *trans* pH was lowered. This suggests that the protonation-induced Cl^- flow generates a *cis*-to-*trans* electroosmotic flow at a positive voltage, which can drive DNA into the pore from the *cis* entrance (Fig. 1a model). Similarly, lowering *cis* pH can result in an opposite *trans*-to-*cis* electroosmotic flow under a negative voltage, enabling aerolysin to capture DNA presented in the *trans* solution (Fig. S4 model). The electroosmotic effect is also supported by the observation that the DNA capture rate is linearly increased with the voltage (Fig. 1b). This is consistent with the linear voltage-dependence of the electroosmotic flow as determined by the Helmholtz–Smoluchowksi equation[46], and that the capture rate is proportional to the water flow velocity that is increased linearly with the voltage applied[45].

Fig. 3b (bottom) also shows that the net Cl^- flow reached the maximal level around pH3.0 (J/J_0 =95% at *trans* pH3.2). Beyond pH3.0, the electroosmotic effect becomes saturated, but the capture rate continued to increase. One possibility is that very low *trans* pH may even "remotely" protonate residues at the *cis* entrance (e.g. D209 and D216) through a $[H^+]$ gradient across the pore. Upon protonation, the local positively charged residues (e.g. R220, R282 and R288) could attract DNA in the bulk solution. To protonate the *cis* entrance D209 and D216 (pKa=3.86), the *trans* pH must be lower than this pKa due to a pH gradient along the pore. This is consistent with the experiment result that the k_{on}–*trans* pH curve (Fig. 3b) gave pH_{50}=3.2, lower than pKa=3.86. In addition, we lowered *cis* pH to 3.4 (*trans* pH remained 7.4) and observed *cis* DNA capturing blockades (Fig. S8), verifying that the protonated *cis* entrance carrying positive charges can enhance DNA capturing. Moreover, placing charged motif at the protein pore entrance has been found to enhance DNA capture efficiency[47] and is a key design parameter that needs fulfilling to optimize the biosensing performance[48].

In summary, we have discovered a remote pH modulation mechanism to transform aerolysin into a highly nucleic acids-sensitive nanopore for potential genetic detection. This method is efficient, while simple and easy to operate, and the resulting deceleration of DNA translocation is a desired property for both sequencing and precise genetic detection. In addition, this method is also applicable to other nanopore system (Fig. S9). Most importantly, unlike previous work in which pH of both sides were changed (for α-hemolysin)[41], our method keeps the target gene fragments in the neutral environment throughout the detection, therefore effectively preventing target nucleic acids from chemical damaging. In particular, this advantage is critical for preserving the structure of nucleic acids (e.g. RNA tertiary structure). This method may ignite new studies on nanopore sensing mechanism. Guided by the structure[43], we can engineer the aerolysin pore with different charge distributions to mimic the protonation mechanism and to improve biosensing performance. We can also adapt this method to detection of genetic alteration such as circulating nucleic acids biomarkers[49-51] and molecular processes like tertiary unfolding mechanism and nucleic acids-ligand interactions.

ASSOCIATED CONTENT

Supporting Information

The Supporting Information is available free of charge on the ACS Publications website. Sequences, pKa, *I*–*t* scattering plot, *f*–[DNA] and k_{on}–[DNA] curves, *I*–pH curve, RNA translocation, ion selectivity measurement, PCR result, τ histograms, DNA charge evaluation, supplementary methods.

AUTHOR INFORMATION

Corresponding Authors

*E-mail: ywan1012@asu.edu or gul@missouri.edu
ORCID
Li-Qun Gu: 0000-0002-8710-6160

ACKNOWLEDGEMENTS

We are grateful to the National Institutes of Health for support of this work through GM114204 and HG009338.

REFERENCES

1. Howorka, S., Siwy, Z., *Chem Soc Rev* **2009**, *38*, 2360-84.
2. Kasianowicz, J. J., Robertson, J. W., Chan, E. R., Reiner, J. E., Stanford, V. M., *Annu Rev Anal Chem (Palo Alto Calif)* **2008**, *1*, 737-66.
3. Cherf, G. M., Lieberman, K. R., Rashid, H., Lam, C. E., Karplus, K., Akeson, M., *Nat Biotechnol* **2012**, *30*, 344-348.
4. Laszlo, A. H., Derrington, I. M., Ross, B. C., Brinkerhoff, H., Adey, A., Nova, I. C., Craig, J. M., Langford, K. W., Samson, J. M., Daza, R., Doering, K., Shendure, J., Gundlach, J. H., *Nat Biotechnol* **2014**.
5. Rhee, M., Burns, M. A., *Trends Biotechnol* **2006**, *24*, 580-6.
6. Clarke, J., Wu, H. C., Jayasinghe, L., Patel, A., Reid, S., Bayley, H., *Nat Nanotechnol* **2009**, *4*, 265-70.
7. Derrington, I. M., Butler, T. Z., Collins, M. D., Manrao, E., Pavlenok, M., Niederweis, M., Gundlach, J. H., *Proc Natl Acad Sci U S A* **2010**, *107*, 16060-5.
8. Ying, Y. L., Zhang, J., Gao, R., Long, Y. T., *Angew Chem Int Ed Engl* **2013**, *52*, 13154-61.
9. Wang, Y., Tian, K., Lehr, H., Ritzo, B., Gu, L.-Q., *Nanoscale* **2014**.
10. Wang, Y., Luan, B.-Q., Yang, Z., Zhang, X., Ritzo, B., Gates, K., Gu, L.-Q., *Scientific reports* **2014**, *4*.
11. Movileanu, L., *Soft Matter* **2008**, *4*, 925-931.
12. Bikwemu, R., Wolfe, A. J., Xing, X., Movileanu, L., *Journal of Physics Condensed Matter* **2010**, *22*.
13. Rosen, C. B., Rodriguez-Larrea, D., Bayley, H., *Nat Biotechnol* **2014**, *32*, 179-81.
14. Wolfe, A. J., Mohammad, M. M., Cheley, S., Bayley, H., Movileanu, L., *J Am Chem Soc* **2007**, *129*, 14034-41.
15. Rotem, D., Jayasinghe, L., Salichou, M., Bayley, H., *J Am Chem Soc* **2012**, *134*, 2781-7.
16. Wang, S., Haque, F., Rychahou, P. G., Evers, B. M., Guo, P., *ACS Nano* **2013**, *7*, 9814-22.
17. Rodriguez-Larrea, D., Bayley, H., *Nature Nanotechnology* **2013**, *8*, 288-295.
18. Oukhaled, G., Mathe, J., Biance, A. L., Bacri, L., Betton, J. M., Lairez, D., Pelta, J., Auvray, L., *Phys Rev Lett* **2007**, *98*, 158101.
19. Goodrich, C. P., Kirmizialtin, S., Huyghues-Despointes, B. M., Zhu, A., Scholtz, J. M., Makarov, D. E., Movileanu, L., *Journal of Physical Chemistry B* **2007**, *111*, 3332-3335.
20. Mereuta, L., Roy, M., Asandei, A., Lee, J. K., Park, Y., Andricioaei, I., Luchian, T., *Scientific Reports* **2014**, *4*.
21. Stefureac, R., Long, Y. T., Kraatz, H. B., Howard, P., Lee, J. S., *Biochemistry* **2006**, *45*, 9172-9.
22. Cressiot, B., Braselmann, E., Oukhaled, A., Elcock, A. H., Pelta, J., Clark, P. L., *ACS nano* **2015**, *9*, 9050-9061.
23. Pastoriza-Gallego, M., Rabah, L., Gibrat, G., Thiebot, B., van der Goot, F. G., Auvray, L., Betton, J. M., Pelta, J., *J Am Chem Soc* **2011**, *133*, 2923-31.
24. Payet, L., Martinho, M. n., Pastoriza-Gallego, M., Betton, J.-M., Auvray, L., Pelta, J., Mathé, J. r. m., *Analytical chemistry* **2012**, *84*, 4071-4076.
25. Merstorf, C. l., Cressiot, B., Pastoriza-Gallego, M., Oukhaled, A., Betton, J.-M., Auvray, L., Pelta, J., *ACS chemical biology* **2012**, *7*, 652-658.
26. Stefureac, R., Waldner, L., Howard, P., Lee, J. S., *Small* **2008**, *4*, 59-63.
27. Wang, Y., Montana, V., Grubišić, V., Stout, R. F., Parpura, V., Gu, L. Q., *ACS Applied Materials and Interfaces* **2015**, *7*, 184-192.
28. Fennouri, A., Daniel, R. g., Pastoriza-Gallego, M., Auvray, L., Pelta, J., Bacri, L., *Analytical chemistry* **2013**, *85*, 8488-8492.
29. Baaken, G., Halimeh, I., Bacri, L., Pelta, J., Oukhaled, A., Behrends, J. C., *ACS nano* **2015**, *9*, 6443-6449.
30. Kasianowicz, J. J., Brandin, E., Branton, D., Deamer, D. W., *Proc Natl Acad Sci U S A* **1996**, *93*, 13770-3.
31. Wang, H. Y., Li, Y., Qin, L. X., Heyman, A., Shoseyov, O., Willner, I., Long, Y. T., Tian, H., *Chem Commun (Camb)* **2013**, *49*, 1741-3.
32. Pastoriza-Gallego, M., Breton, M. F., Discala, F., Auvray, L., Betton, J. M., Pelta, J., *ACS Nano* **2014**, *8*, 11350-60.
33. Payet, L., Martinho, M., Merstorf, C., Pastoriza-Gallego, M., Pelta, J., Viasnoff, V., Auvray, L., Muthukumar, M., Mathe, J., *Biophys J* **2015**, *109*, 1600-7.
34. Cao, C., Ying, Y. L., Hu, Z. L., Liao, D. F., Tian, H., Long, Y. T., *Nat Nanotechnol* **2016**, *11*, 713-8.
35. Wang, Y., Zheng, D., Tan, Q., Wang, M. X., Gu, L. Q., *Nat Nanotechnol* **2011**, *6*, 668-74.
36. Muthukumar, M., *J Chem Phys* **2010**, *132*, 195101.
37. Wanunu, M., Morrison, W., Rabin, Y., Grosberg, A. Y., Meller, A., *Nature Nanotechnology* **2010**, *5*, 160-165.
38. Rowghanian, P., Grosberg, A. Y., *Physical Review E* **2013**, *87*, 042722.
39. Squires, A., Meller, A., *Biophys J* **2013**, *105*, 543-4.
40. Tian, K., He, Z., Wang, Y., Chen, S. J., Gu, L. Q., *ACS Nano* **2013**, *7*, 3962-9.
41. de Zoysa, R. S., Krishantha, D. M., Zhao, Q., Gupta, J., Guan, X., *Electrophoresis* **2011**, *32*, 3034-41.
42. Wang, Y., Montana, V., Grubisic, V., Stout, R. F., Jr., Parpura, V., Gu, L. Q., *ACS Appl Mater Interfaces* **2015**, *7*, 184-92.
43. Degiacomi, M. T., Iacovache, I., Pernot, L., Chami, M., Kudryashev, M., Stahlberg, H., van der Goot, F. G., Dal Peraro, M., *Nat Chem Biol* **2013**, *9*, 623-9.
44. Iacovache, I., De Carlo, S., Cirauqui, N., Dal Peraro, M., van der Goot, F. G., Zuber, B., *Nat Commun* **2016**, *7*, 12062.
45. Gu, L. Q., Cheley, S., Bayley, H., *Proc Natl Acad Sci U S A* **2003**, *100*, 15498-503.
46. Bard, A. J., Faulkner, L. R., Leddy, J., Zoski, C. G., *Electrochemical methods: fundamentals and applications*. Wiley New York: 1980; Vol. 2.
47. Maglia, G., Restrepo, M. R., Mikhailova, E., Bayley, H., *Proceedings of the National Academy of Sciences of the United States of America* **2008**, *105*, 19720-19725.
48. Capone, R., Blake, S., Restrepo, M. R., Yang, J., Mayer, M., *Journal of the American Chemical Society* **2007**, *129*, 9737-9745.
49. Calin, G. A., Croce, C. M., *Nat Rev Cancer* **2006**, *6*, 857-66.
50. Vlassov, V. V., Laktionov, P. P., Rykova, E. Y., *Curr Mol Med* **2010**, *10*, 142-65.
51. Mitchell, P. S., Parkin, R. K., Kroh, E. M., Fritz, B. R., Wyman, S. K., Pogosova-Agadjanyan, E. L., Peterson, A., Noteboom, J., O'Briant, K. C., Allen, A., Lin, D. W., Urban, N., Drescher, C. W., Knudsen, B. S., Stirewalt, D. L., Gentleman, R., Vessella, R. L., Nelson, P. S., Martin, D. B., Tewari, M., *Proc Natl Acad Sci U S A* **2008**, *105*, 10513-8.

TOC